

ICANS-VI
INTERNATIONAL COLLABORATION ON ADVANCED NEUTRON SOURCES
June 27 - July 2, 1982

eV NEUTRON SPECTROSCOPY USING RESONANCE ABSORPTION ENERGY
SELECTION ON A PULSED SOURCE

W G Williams and J Penfold
Neutron Division, Rutherford Appleton Laboratory

ABSTRACT

A method is proposed for measuring excitation energies up to approx 1 eV by using an absorption foil difference technique in the inverse geometry. The discussion is restricted to using the ^{149}Sm resonance at an energy $E_R = 0.873$ eV and utilises other fixed absorption filters to improve the sensitivity of the method for inelastic measurements. Feasibility tests have been carried out on the LAD total scattering spectrometer at the Harwell Linac. By extrapolating from results obtained for ZrH_2 it is predicted that with more powerful sources such as the SNS it should be possible to observe high energy magnetic excitations.

eV NEUTRON SPECTROSCOPY USING RESONANCE ABSORPTION ENERGY
SELECTION ON A PULSED SOURCE

W G Williams and J Penfold

Neutron Division, Rutherford Appleton Laboratory

1. INTRODUCTION

The new pulsed neutron sources provide much greater fluxes of epithermal neutrons than steady state sources and the importance of this characteristic to studies in condensed matter physics has been expounded by several authors eg Sinha⁽¹⁾. In order to exploit this feature in dynamical studies we require effective monochromators at neutron energies $E \gtrsim 1\text{eV}$ and three methods of energy selection viz (i) crystal monochromators⁽²⁾, (ii) phased Fermi choppers⁽³⁾ and (iii) nuclear resonance absorption⁽⁴⁾ may be considered. A detailed discussion of methods (i) and (ii) has been given in reference 2; they provide a means of performing high resolution measurements (energy transfer resolutions $\Delta\hbar\omega/\hbar\omega \sim 2\%$).

Two variations of method (iii) have been examined. In the first, the "resonance detector spectrometer"^(4,5,6), an analysing foil placed after the scatterer captures neutrons resonantly over a narrow energy region and the emitted γ -rays are detected. This is an example of an inverse geometry instrument in which a large fraction of the incident white pulsed beam can be utilised. The second variation is a direct geometry instrument, the "filtered beam spectrometer"⁽⁷⁾, where the absorbing foil is used to define the incident neutron energy and the difference TOF spectra of data collected with and without the foil gives the sample's response to the resonance energy incident neutrons.

This paper discusses the possibilities of using a Samarium-149 resonance absorber with a resonance energy $E_R = 0.873$ eV for inelastic experiments initially at the Harwell Linac and later on the SNS. The reason for confining the discussion to this resonance is two-fold: (i) it is possible to polarise the nucleus⁽⁸⁾, so there is the potential eventually of extending the method to look at spin-dependent scattering processes, and (ii) the resonance has a conveniently small total width $\Gamma = 60$ meV⁽⁹⁾. It was decided first to examine the possibilities offered by the foil difference method, both in direct and inverse instrument geometries. In the latter case, in contrast to ref 7, the difference TOF spectra result from scattered neutrons at the resonance energy.

2. FOIL DIFFERENCE METHOD IN DIRECT AND INVERSE GEOMETRIES

Since the difference counts are always combined with the total TOF on a pulsed source spectrometer it is possible, at least in principle, to use the foil difference technique in either the direct or inverse geometry. The advantages and disadvantages of each method can only really be assessed by experiment, however for foils with $E_R \sim 1$ eV such as Sm, we favour using the inverse geometry approach. The need to carry out many measurements at the lowest possible momentum transfer $\hbar Q$ means that the scattered neutron wavevector k_2 (hence energy E_2) should be as high as possible; this is easiest with $E_2 = E_R$ for neutron down-scattering ie with an analyser foil after the scatterer.

Another important reason for choosing the inverse geometry is that it should in practice provide better energy resolution over much of the energy transfer range of interest ($0.2 < \hbar\omega(\text{eV}) < 1$). These resolutions are dominated by the term representing the energy width of the resonance peak and for direct (D) and inverse (I) geometry spectrometers on a pulse source may be approximated by:

$$\left[\frac{\Delta \hbar \omega}{\hbar \omega} \right]_I = \frac{\Delta E_R}{\hbar \omega} \left[1 + \frac{L}{L_1} \left(\frac{E_1}{E_R} \right)^{1.5} \right], \quad \text{and} \quad (2.1)$$

$$\left[\frac{\Delta \hbar \omega}{\hbar \omega} \right]_D = \frac{\Delta E_R}{\hbar \omega} \left[1 + \frac{L}{L_2} \left(\frac{E_2}{E_R} \right)^{1.5} \right] \quad (2.2)$$

where L_1 and L_2 represent the incident and scattered beam flight paths, and E_1 and E_2 the incident and scattered neutron energies. We now calculate these contributions to the energy resolutions for situations where the difference count rates (per unit energy transfer) in the direct and inverse geometry foil experiments are comparable. Matching of incident and scattered beam solid angles gives:

$$\left[\frac{A_m}{L_1^2} \cdot \frac{A_d}{L_2^2} \right]_D = \left[\frac{A_m}{L_1^2} \cdot \frac{A_d}{L_2^2} \right]_I \quad (2.3)$$

where A_m and A_d are the moderator and total detector areas and if we assume that these are equal (it should for example be possible to cover a large part of the scattered beam solid angle by placing the absorbing foil close to the sample in case I) we obtain equivalent count rate differences with:

$$\begin{aligned} (L_1 L_2)_D &= (L_1 L_2)_I, \quad \text{or} \\ L_1 D L_2 D &= L_1 I D_2 I \end{aligned} \quad (2.4)$$

The resolution equations require $L_{2I} \ll L_{1I}$ and $L_{2D} \gg L_{1D}$, and whereas the first condition is relatively easily met, the second is not. For the SNS L_{1D} must be greater than approx 6 m so that the sample extends beyond the biological shielding. We have calculated the energy resolutions for the following hypothetical (but practical) spectrometer case where equation (2.4) is fulfilled:

$$\begin{aligned} L_{1D} &= 6 \text{ m}; & L_{2D} &= 3 \text{ m} \\ L_{1I} &= 18 \text{ m}; & L_{2I} &= 1 \text{ m} \\ \text{and } E_R &= 1 \text{ eV}; & \Delta E_R &= 0.05 \text{ eV} \end{aligned}$$

The results are shown in Figure 1. It is concluded that the inverse geometry arrangement gives appreciably better resolutions for resonance energy foils with $E_R \sim 1$ eV and it was decided to carry out detailed calculations of the performance of a Sm analyser difference spectrometer on the Harwell Linac and SNS sources.

The equating of luminosities, as discussed above, neglects the effect of the incident and scattered beam divergencies on the Q resolution. This factor was considered, at least initially, to be less important than the optimisation of the intensity and energy transfer resolution. The beam divergence effect on the Q resolution can, in principle, be improved by reducing the area of detector elements while maintaining large total areas.

3. ENERGY SELECTION USING THE SAMARIUM RESONANCE AT $E_R = 0.873$ eV

The optimum resolutions and difference counts in resonance absorption difference spectrometers are obtained by optimising the thickness of the absorption foil. If the foil is too thin the difference counts are less than the optimum, whereas very thick foils cause a degradation in the energy transfer resolutions. The optimisation method described in this section was applied to the Sm resonance at $E_R = 0.873$ eV. It has been shown⁽¹⁰⁾ that the absorption cross-section across this resonance peak can be described by the Breit Wigner expression:

$$\sigma(E) = \left(\frac{\sigma_0}{1 + 4(E-E_R)^2/\Gamma^2} \right)^{\frac{1}{2}} \left(\frac{E}{E_R} \right)^{\frac{1}{2}} \quad (3.1)$$

where E is the neutron energy, Γ the total resonance width, and σ_0 is the maximum cross-section at the resonance energy E_R . The foil attenuation $A(E)$ across the absorption peak, which is proportional to the difference counts in these experiments, is then given by:

$$A(E) = 1 - \exp \left\{ \frac{-\sigma Nd}{1 + 4(E-E_R)^2/\Gamma^2} \left(\frac{E}{E_R} \right)^{\frac{1}{2}} \right\}, \quad (3.2)$$

where Nd is the atomic thickness of the absorbing nucleus in the foil. This function was calculated for the Sm resonance using the recommended resonance parameters given in reference (9). The curves for different Sm thicknesses Nd are shown in Fig 2. The foil thickness optimisation uses a quality factor $A(E_R)/\Delta E_R^2$, where $A(E_R)$ is the attenuation factor at $E = E_R$ and ΔE_R is the FWHM of the attenuation peak. The variation of this quality factor with Sm foil thickness is also shown in Fig 2. We conclude that the optimum Sm thickness is $Nd \sim 3.5 \times 10^{20}$ at cm^{-2} . In the calculations to be presented and in the test experiments to be performed we shall use a Sm foil atomic thickness $Nd \sim 3.0 \times 10^{20}$ at cm^{-2} which corresponds to a physical thickness $d \sim 0.1$ mm; this gives a peak attenuation $A(E_R) = 0.61$ and a resolution width $\Delta E_R = 0.075$ eV.

4. DESIGN OF RESONANCE FILTER DIFFERENCE SPECTROMETER IN THE INVERSE GEOMETRY

(a) Outline Description

Feasibility experiments on the resonance foil analyser method were carried out on the SNS total scattering spectrometer LAD⁽¹¹⁾ which is currently in operation at the Harwell Linac. This has convenient incident ($L_1 = 10.5$ m) and scattered ($L_2 = 1$ m) neutron flight paths to give a near optimum resolution in inverse geometry. Detectors at scattering angles $\theta = 5^\circ, 10^\circ$ and 20° were used and the detector apertures were opened up to approx 20 mm (wide) x 250 mm (high); these are considerably larger than that normally used in the high Q resolution mode. We were particularly interested in the performance of the instrument at small scattering angles since its application to magnetic scattering problems demands a low Q capability. Figure 3 shows a schematic diagram of the test instrument. The functions of the incident and scattered beam absorption filters are described in the following section.

(b) Incident and Scattered Beam Filters

The statistical errors in the filter difference method for measuring inelastic scattering processes can be considerably reduced by minimising the general background in the spectrometer as well as the counts due to elastic scattering. This is achieved in this spectrometer design by using two sets of absorbing filters, one in the incident beam and one in the scattered beam; these remain stationary in all measurements. The purpose of the incident beam filter (Filter A) is to selectively attenuate neutrons of energies $E \leq 1$ eV and this contains Cd, Er and Sm absorbers. The Sm filter is the highest energy

absorber of these three and is made "thick" to ensure that no $E = 0.873$ eV neutrons are incident at the scatterer. This means that any 0.873 eV neutrons detected by the Sm foil analyser difference method must have been scattered inelastically, in fact by down-scattering. The thermal neutron absorbers (Cd and Sm) also serve to remove potential "frame overlap" slow neutrons from the incident beam. For example elastically scattered neutrons at energies 12 - 13 meV arising from the previous machine pulse would also appear in the same time channels as the main inelastic events of interest in the LAD test instrument. The second set of filters (Filter B) contains Hf, In and Rh foils and is placed in the scattered beam to reduce the counts detected due to elastic scattering at neutron energies between approx 1.1 eV and 1.6 eV. The compositions of filters A and B are given in Table 1 and their calculated transmittances at neutron energies up to 1.8 eV are illustrated in Fig 4. It is reiterated that their function is to reduce the number of counts that occur in the time channels where a difference count due to inelastic scattering can be expected ie they improve the sensitivity of the difference method but do not contribute to the difference count.

Filters	Atomic Thickness of Absorber (at cm^{-2})	Physical Thickness
Filter A { Cd Er ₂ O ₃ Powder Sm ₂ O ₃ Powder	9.3 x 10 ²¹ 1.0 x 10 ²² (Er) 9.2 x 10 ²¹ (Sm)	2 mm 15 mm 30 mm
Filter B { In foil Rh foil Hf foil	1.9 x 10 ²¹ 3.6 x 10 ²⁰ 1.1 x 10 ²¹	0.5 mm 0.05 mm 0.25 mm

Table 1 Incident and scattered beam filters used for Sm foil analyser instrument tests.

It is worthwhile expanding on the discrimination between elastic and inelastic events provided by the incident and scattered beam filters. The transmittance product $T_A T_B$ is shown as a function of total time-of-flight on the test instrument for both elastic and inelastic scattering in Fig 5. The difference counts are proportional to $T_A T_B$ (inel) whereas $T_A T_B$ (el) produces a constant "background" count in the two parts of the measurement. The elastic-inelastic discrimination is particularly good for energy transfers between 0.4 and 0.9 eV.

(c) Predicted Performance of Test Instrument

The expected performance of the test instrument was simulated using a computer code written by R M Richardson for the Beryllium Filter inverse geometry spectrometer on the SNS⁽¹²⁾ which has been modified for resonance peak analysers. The code predicts the energy transfer and momentum transfer resolutions by including all the possible contributions due to uncertainties in lengths and times as well as the spread in the energy selection. It also gives the count rates where the scattering cross-section is well known or can be modelled.

Fig 6 shows the energy transfer resolution $\Delta\hbar\omega/\hbar\omega$, which is effectively determined by the absorption peak width $\Delta E_R = 0.075$ eV, calculated for the test instrument as a function of the energy transfer. Fig 7 shows the (Q, ω) scans available on the test instrument for the three fixed angle detectors at $\theta = 5^\circ, 10^\circ$ and 20° . The Q difference offered by the three detector scans may be useful in distinguishing between nuclear and magnetic inelastic scattering, though this will probably require a smaller 5° detector height (approx 100 mm) ie improved Q resolution. The figure also shows that it should be possible to observe magnetic excitations up to energies $\hbar\omega \sim 0.35$ eV with the 5° detector ($Q \ll 4\text{\AA}^{-1}$).

Figure 8 shows a simulation of the time of flight spectra with and without the analysing foil for an isotropic Einstein oscillator with unit effective mass (eg H in a metal) where the fundamental frequency is $\hbar\omega_0 = 0.16$ eV. The sample chosen was a 25% scatterer and the predicted count rates pertain only to the 5° detector on the LAD test instrument where the inelastic cross-section for the fundamental mode was estimated to be $(d^2\sigma/d\Omega dE) \sim 2.3$ barns $\text{sr}^{-1} \text{eV}^{-1}$. The difference count rates are also shown in the figure and the integrated difference count rate over the fundamental peak is approx 10 cts/hr. The two most important features to notice are: (i) that the

difference count rates are always larger than a factor $\times 0.1$ compared with the individually measured count rates over the major part of the energy transfer range of interest ($\hbar\omega \approx 1$ eV) and (ii) the difference counts at times of flight ~ 970 μsec correspond to elastically scattered neutrons at energies ~ 0.73 eV, where there is an increase in the transmittance of the incident beam filters (see T_A curve in Fig 4).

These count rate calculations were also substantiated using analytic expressions similar to those given by Allen et al⁽⁴⁾ for the resonance detector spectrometer. The predicted count rates for the other two detectors were approximately $\times 2$ those shown for the 5° detector.

(d) Measurements with a ZrH₂ scatterer

The raw data T.O.F. difference spectra due to hydrogen vibrations in a zirconium hydride 25% scattering sample on the LAD Test spectrometer are shown in Figs 9(a-c). The fundamental mode at $\hbar\omega = 0.14$ eV and the overtone modes are clearly observed, though they remain unresolved due largely to the Doppler broadening of the resonance absorption peak which was not included in the computer simulation. The variation in the peak intensities at different scattering angles has the expected Q-dependence. These preliminary results clearly demonstrate the feasibility of the experimental method.

5. SUMMARY

A discussion has been presented of the application of a resonance absorber difference method in an inverse geometry TOF spectrometer for measuring excitations over the energy transfer range $0.1 < \hbar\omega$ (eV) < 1 . The feasibility of the technique was assessed using the LAD total scattering spectrometer at the Harwell Linac as a test instrument. It should prove possible to use the method to observe overtone modes in metal-hydrogen samples, and, particularly with more powerful sources such as the SNS, high energy magnetic excitations.

Finally it should be pointed out that significant improvements in these count rates are expected for any purpose-designed SNS instrument since:

- (i) large improvements in the detector solid angle ($\times 10$) should easily be possible, and

(ii) the SNS source strength at full intensity is approx x600 that used in above calculations and experiment.

It is therefore reasonable to expect any SNS instrument to be capable of measuring cross-sections at least three orders of magnitude lower than that given in the above example, and this brings with it the prospect of observing many magnetic excitations which have hitherto not been measureable.

ACKNOWLEDGEMENT

The authors acknowledge useful discussions with our colleagues Dr R Cywinski and Dr A D Taylor.

REFERENCES

1. S K Sinha. J Appl Phys 50 (1979) 1952
2. C J Carlile and W G Williams. ' Inelastic Neutron Scattering using a Crystal Spectrometer on a Pulsed Source'. Rutherford Appleton Laboratory Report RL-81-028 (1981)
3. B C Boland 'High Energy Inelastic Spectrometer'. Proc ICANS-IV KENS Report II (1981) 580
4. D R Allen, E W J Mitchell and R N Sinclair. J Phys E Sci Instrum 13 (1980) 639
5. R N Sinclair, M C Moxon and J M Carpenter. Bull Am Phys Soc 22 (1977) 101
6. L Cser, N Kroo, P Pacher, V G Simkin and E V Vasilyeva. Nucl Instrum Meth 179 (1981) 515
7. R M Brugger, A D Taylor, C E Olsen and J A Goldstone. Bull Am Phys Soc 27 (1982) 14
8. F F Freeman and W G Williams. J Phys E Sci Instrum 11 459 (1978)
9. 'Neutron Cross Sections'. BNL 325 Second Edition Supplement No: 2. August 1966 62-149-3
10. A W McReynolds and E Andersen Phys Rev 93 (1954) 195
11. W S Howells. 'A Diffractometer for Liquid and Amorphous Materials Research'. Rutherford Appleton Laboratory Report RL-80-017 (1980)
12. R M Richardson. 'A High Throughput Inelastic Neutron Scattering Spectrometer for the Harwell Linac and the Spallation Neutron Source'. Rutherford Appleton Laboratory Report RL-82-035 (1982).

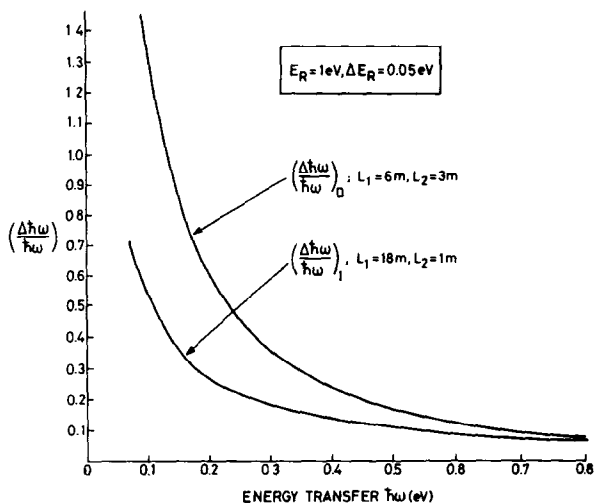


Fig. 1. Energy transfer resolutions in direct(D) and inverse(I) geometry resonance absorption spectrometers.

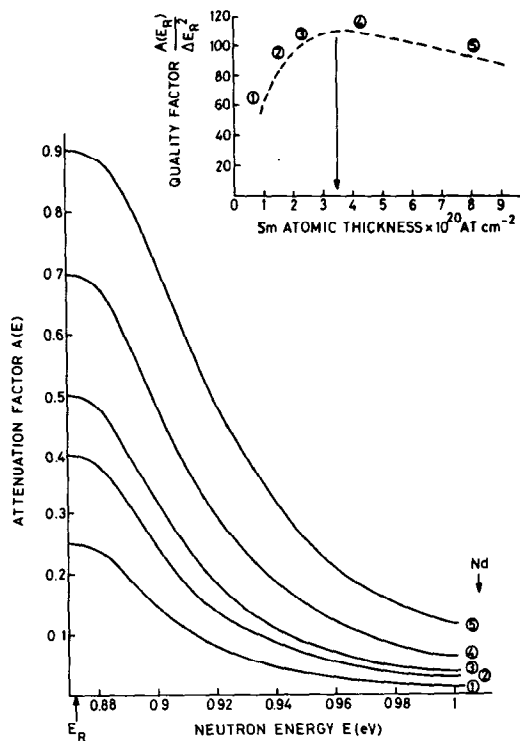


Fig. 2. Attenuation curves for different Sm atomic thicknesses around $E_R = 0.873eV$.

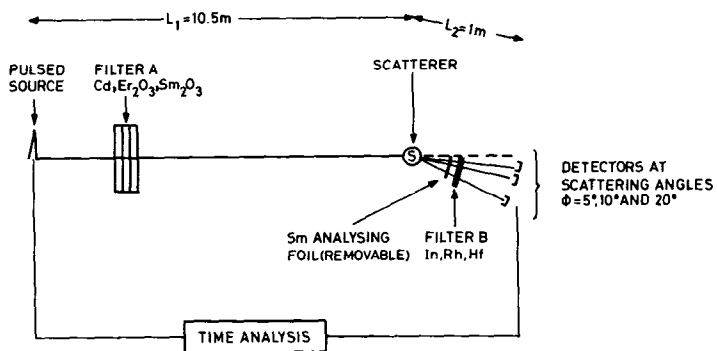


Fig. 3

Schematic diagram of resonance foil difference method in the inverse geometry on a pulsed source (the distances and detectors shown are those used in the Lad test experiments).

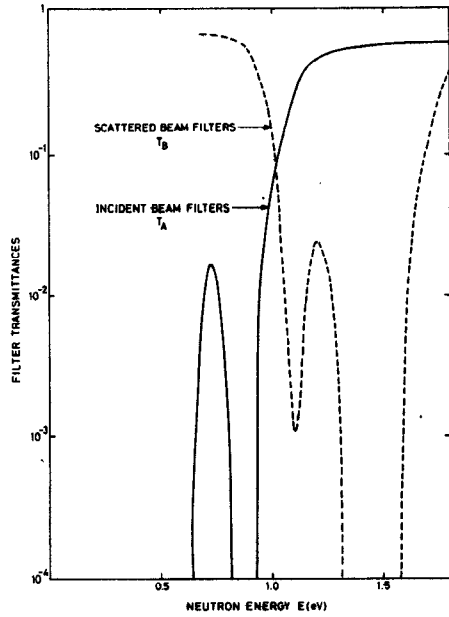


Fig. 4. Neutron energy dependences of the transmittances of the incident and scattered beam filters.

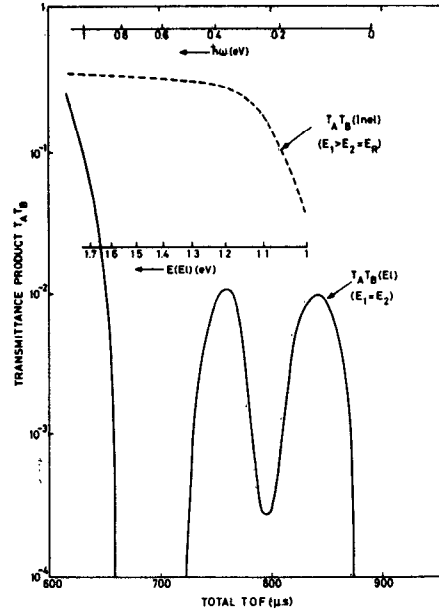


Fig. 5. Elastic-inelastic scattering discrimination provided by incident and scattered beam filters.

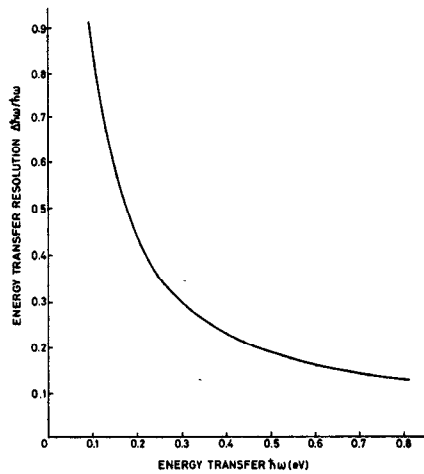


Fig. 6. Energy transfer resolution on Lad test instrument.

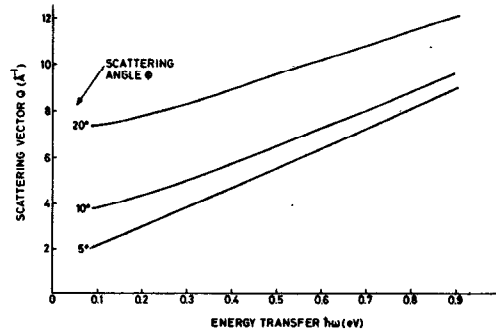


Fig. 7. (Q, ω) Scans on Lad test instrument for fixed angle detectors at $\phi = 5^\circ, 10^\circ$ and 20° .

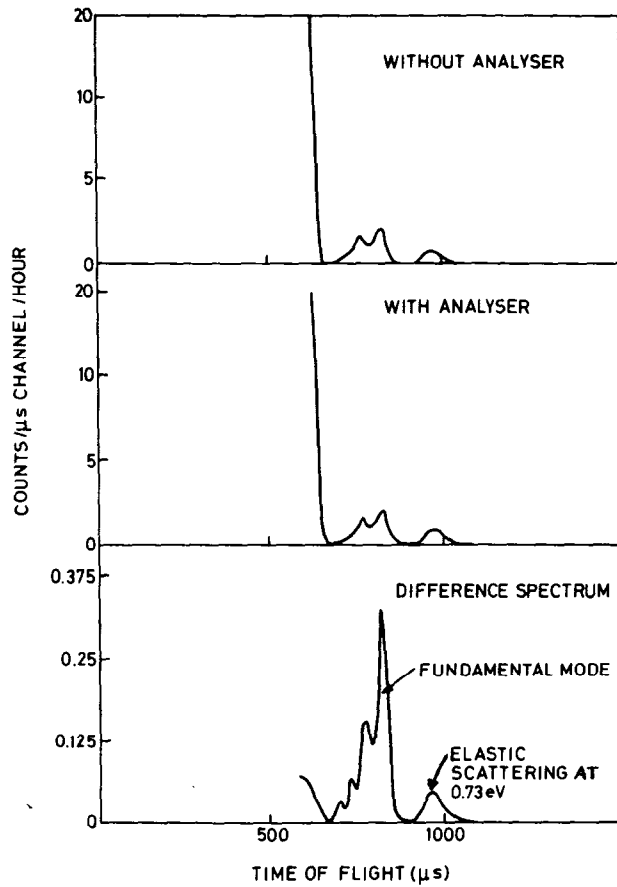


Fig. 8

Simulated T.O.F. spectra for a 25% metal hydride scatterer with fundamental frequency $\hbar\omega_0 = 0.16\text{eV}$ on the Lad test instrument.

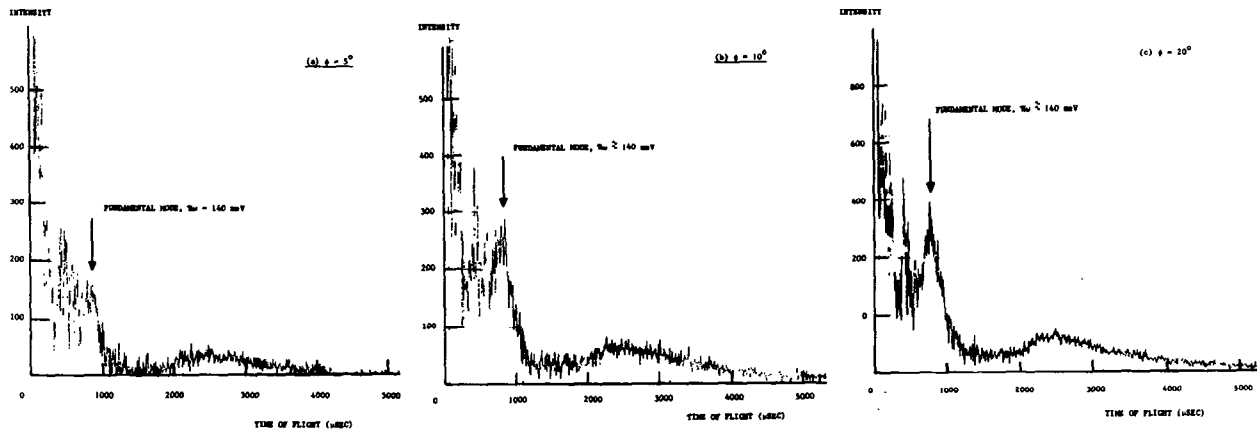


Fig. 9. T.O.F. difference spectra for a 25% ZrH_2 scatterer on the Lad test instrument.